(Received 22 October 2025, Accepted 08 December 2025, Scheduled 18 December 2025)

Robust Adaptive Array Beamforming Using Generalized Sidelobe Canceller and Zero-forcing Equalizer under Array Mutual Coupling

Cheng-Jie Wang[1] and Ju-Hong Lee[2,*]

[1]Graduate Institute of Communication Engineering, National Taiwan University, Taiwan
[2]Department of Electrical Engineering, Graduate Institute of Communication Engineering, National Taiwan University, Taiwan

ABSTRACT: Generalized sidelobe canceller (GSC) based adaptive beamformer possesses a main advantage of superior interference rejection due to its capability in tracking the interference characteristics. However, its performance is very sensitive to even a small mismatch in array scenarios. For example, the mismatch due to mutual coupling between array sensors is a common phenomenon in practical environments. Two common problems considered are as follows. (1) The existing adaptive array beamformers are very sensitive to MCE. (2) The existing robust methods inevitably suffer from the problems, including additional computational complexity and estimate accuracy. In this paper, we present an efficient method to deal with the performance degradation induced by the MCE to achieve robust beamforming. The proposed method simply utilizes a well-known scheme, namely the zero-forcing (ZF) equalizer. The ZF equalizer simply preprocesses the data vector received by the antenna array and then inputs the processed data vector into a GSC based adaptive array processor. The combination of a ZF equalizer and a GSC based adaptive array processor results in an adaptive array beamformer providing satisfactory beamforming performance in the presence of the MCE. The performance analysis regarding the proposed method is analyzed. Simulation results are also presented for confirmation and comparison. The simulation results show that the ZF equalizer alleviates the MCE and the GSC based adaptive beamformer can subdue the background noise enhanced by ZF equalizer.

1. INTRODUCTION

Adaptive beamforming is widely considered in the radar [1], atmosphere [2], sonar [3], more recently, wireless communications [4, 5]. Adaptive array beamforming is usually considered based on the criteria of linearly constrained minimum variance (LCMV) [6] because of capabilities in suppressing interference signals and noise. By contract, generalized sidelobe canceller (GSC) [7] provides the same performance as LCMV [8] and offers several advantages over the LCMV [9–11]. However, LCMV and GSC suffer deterioration of performance due to scenario mismatches. For instance, a common phenomenon in practical environments is mutual coupling (MC) between array sensors. The MC comes from the electromagnetic interactions between the array sensors and has been widely concerned in the literature [12, 13].

For years, solving the MCE has attracted much endeavor and resulted in many achievements reported in the literature. Notable among them are reviewed as follows. [14] simply considers the theory based on electromagnetic concept with a known MC matrix and uses a basic compensation algorithm to deal with the MCE. However, this method can only be used in the cases when the MC coefficients are exactly known. Recently, many robust methods were presented for curing the MC problem. We briefly describe some notable of them as follows. The method of [15] optimally estimates the direction vectors of the interference signals to construct an interference-plus-noise correlation matrix required for beamforming through an optimization approach. The method of [16] utilizes an optimization process to sequentially estimate the MC coefficients and the direction vectors of interference signals. Then, the method reconstructs the interfence-pulse-noise covariance matrix to achieve robust beamforming. Moreover, [10] presents an advanced GSC (AGSC) based beamforming method without resorting to any optimization algorithms. The basic idea of the AGSC focuses on developing an advanced GSC to effectively eliminate the leakage of the desired signal after signal blocking operation. As to [11], it explores the concept of early late gate synchronization to solve an optimization problem without requiring complicated algorithmic complexity to improve the capability of [10]. In contrast, we present an efficient beamforming system simply composed of a traditional GSC [7] and a well-known zero-forcing (ZF) equalizer [17] in this paper. First, the data vector received by an antenna array is directly inputted into the equalizer. As we know, the principle of using ZF is to eliminate the channel effect and avoid the inter-symbol-interference (ISI) for the desired signal under multipath environment. The individual array suffered from MC is influenced by adjacent elements. From an aspect of view of an array element, it can be seen that each instantly received data is the sum of the adjacent values which contain gain and phase delay due to MC effect. As a result, the MC effect can be viewed as an ISI problem and can be eliminated by ZF equalizer. However, ZF equalizer can mitigate the effect of MC mismatch effectively at the price of enhancing the effect of background noise. Therefore, we fur-

* Corresponding author: Ju-Hong Lee (jhlee@ntu.edu.tw).

ther utilize the conventional GSC based array beamformer to effectively subdue the enhanced noise. As a result, the adaptive array beamformer simply combining a simple ZF equalizer and GSC possesses the capabilities of providing robustness and exceptional performance. Furthermore, the proposed robust array beamformer retains the flexibility for beamforming process without requiring any complicated optimization algorithms to achieve robustness and reserve beamforming performance. The performance regarding the proposed method is analyzed. Finally, simulation results are illustrated for comparison and confirmation. The novel achievements of the proposed method are summarized as follows: (1) Without resorting to any complicated optimization algorithms, we utilize the well-known capabilities of ZF equalizer in mitigating the ISI problem to alleviate MCE. (2) The performance of the proposed method is theoretically analyzed. (3) The proposed method simply combines ZF equalizer and conventional GSC based adaptive beamformer to obtain satisfactory robustness and beamforming performance for curing MCE problem. (4) The simulation results show that the idea of treating the MCE as an ISI problem makes the MCE problem tractable.

The rest part of this paper is organized as follows. Section 2 presents the background and introduces signal model for GSC based beamformer. The proposed method is presented in Section 3. The performance analysis is analyzed in Section 4. Numerical results obtained from computer simulations are shown and discussed in Section 5. Finally, we conclude this paper in Section 6.

Notations: The boldface is used for expressing vectors like $\mathbf{a}$ and matrices like $\mathbf{A}$. Scalar a is represented by italic. The superscripts $(\cdot)^T$ and $(\cdot)^H$ denote transpose and Hermitian transpose, respectively. $(\cdot)^*$ represents complex conjugate. $\mathbf{I}_N$ is the identity matrix with size $N \times N$. $\|\mathbf{a}\|$ designates the Euclidean norm of vector $\mathbf{a}$. $\|\mathbf{A}\|_F$ stands for the Frobenius norm of matrix $\mathbf{A}$. $Null(\mathbf{A})$ denotes the null space of matrix $\mathbf{A}$ and $Tr\{\mathbf{A}\}$ the trace of matrix $\mathbf{A}$. $j = \sqrt{-1}$.

2. SIGNAL MODEL AND MATHEMATICAL BACKGROUNDS

2.1. Signal Model

Consider a uniform linear array (ULA) having N isotropic antenna elements. Let the direction angle of a signal be denoted by θ. Then, the corresponding direction vector for a far-field signal can be expressed by

$$\mathbf{a}(\theta) = \begin{bmatrix} 1 & e^{j2\pi\frac{d}{\lambda}\sin(\theta)} & \ldots & e^{j2\pi\frac{(N-1)d}{\lambda}\sin(\theta)} \end{bmatrix}^T, \quad (1)$$

where λ represents the signal wavelength and d denotes the distance between two adjacent antenna elements. As a result, the data vector received by the ULA can be expressed by $\mathbf{x}(t) = \begin{bmatrix} x_1(t) & x_2(t) & \ldots & x_N(t) \end{bmatrix}^T$ and given by

$$\mathbf{x}(t) = s_d(t)\mathbf{a}(\theta_d) + \sum_{j=1}^{P} s_j(t)\mathbf{a}(\theta_j) + \mathbf{n}(t), \quad (2)$$

where P is the number of interference signals. θ_d denotes the direction angle of the desired signal and $\theta_1, \ldots, \theta_P$ represent the direction angles of the P interference signals. $s_d(t)$ and $s_j(t)$, $j = 1, \ldots, P$ represent the desired signal and the jth interference signal, respectively. $\mathbf{n}(t) = \begin{bmatrix} n_1(t) & n_2(t) & \ldots & n_N(t) \end{bmatrix}^T$ is the noise vector and the entries $n_i(t)$, $i = 1, 2, \ldots, N$ are independent identically distributed (i.i.d) random noise components with zero mean and variance σ_n^2. They are mutually uncorrelated with the desired signal. The correlation matrix $\mathbf{R}_{xx} = \mathbb{E}\left\{\mathbf{x}(t)\mathbf{x}(t)^H\right\}$ associated with the received data vector can be expressed by

$$\mathbf{R}_{xx} = \overbrace{\sigma_d^2\mathbf{a}(\theta_d)\mathbf{a}(\theta_d)^H}^{\mathbf{R}_{ss}} + \underbrace{\sum_{j=1}^{P}\sigma_j^2\mathbf{a}(\theta_j)\mathbf{a}(\theta_j)^H + \sigma_n^2\mathbf{I}_N}_{\mathbf{R}_{in}}, \quad (3)$$

where $\mathbf{R}_{ss}$ and $\mathbf{R}_{in}$ represent the correlation matrices associated with the desired signal and the interference-plus-noise, respectively. $\sigma_d^2 = \mathbb{E}\{|s_d(t)|^2\}$ and $\sigma_j^2 = \mathbb{E}\{|s_j(t)|^2\}$ denote the powers of desired signal and the jth interference signal, respectively. The output signal-to-interference-plus-noise ratio (SINR) for evaluating the beamforming performance can be expressed by

$$SINR = \frac{\mathbf{w}^H\mathbf{R}_{ss}\mathbf{w}}{\mathbf{w}^H\mathbf{R}_{in}\mathbf{w}}. \quad (4)$$

2.2. GSC Based Adaptive Beamforming

According to [7], the weight vector of GSC based adaptive beamforming is given by

$$\mathbf{w}_{GSC} = \mathbf{w}_q - \mathbf{B}\mathbf{w}_a, \quad (5)$$

where $\mathbf{w}_q = \frac{1}{N}\mathbf{a}(\theta_d)$ denotes the quiescent weight vector. $\mathbf{B}$ and $\mathbf{w}_a$ represents the signal blocking matrix and adaptive weight, respectively. The columns of $\mathbf{B}$ are constituted by $Null(\mathbf{a}(\theta_d)^H)$. The adaptive weight vector $\mathbf{w}_a$ can be obtained by solving the following optimization problem [7]

$$\min_{\mathbf{w}_a} (\mathbf{w}_q - \mathbf{B}\mathbf{w}_a)^H \mathbf{R}_{xx} (\mathbf{w}_q - \mathbf{B}\mathbf{w}_a). \quad (6)$$

The corresponding solution is given by

$$\mathbf{w}_a = \left(\mathbf{B}^H\mathbf{R}_{xx}\mathbf{B}\right)^{-1}\mathbf{B}^H\mathbf{R}_{xx}\mathbf{w}_q. \quad (7)$$

2.3. Array Mutual Coupling

In the presence of array mutual coupling, the steering vector $\mathbf{a}(\theta)$ is no longer equal to the direction vector of the desired signal. The direction vector can be expressed by

$$\hat{\mathbf{a}}_{MC}(\theta) = \sqrt{N}\frac{\mathbf{C}\mathbf{a}(\theta)}{\|\mathbf{C}\mathbf{a}(\theta)\|}, \quad (8)$$

where $\mathbf{C}$ denotes the mutual coupling (MC) matrix. We employ a typical model [18, 19] regarding the antenna MC to construct the matrix and obtain an MC matrix as follows

$$\mathbf{C} = (Z_A + Z_A^*)(\mathbf{Z} + Z_A^*\mathbf{I}_N)^{-1}, \quad (9)$$

where Z_A is the element's impedance in isolation. For $\frac{\lambda}{2}$ dipole, Z_A value is $73+j42.5(\Omega)$. The (x, y)th entry $z_{x,y}$ of the matrix $\mathbf{Z}$ are given by

$$z_{x,y}=\begin{cases} 30\left\{0.5772+\ln\left(\frac{4\pi}{\lambda}l\right)-C_i\left(\frac{4\pi}{\lambda}l\right)\right\} \\ +30j\left\{S_i\left(\frac{4\pi}{\lambda}l\right)\right\}, & x=y \\ \\ 30\{2C_i\left(u_0\right)-C_i\left(u_1\right)-C_i\left(u_2\right)\} \\ -30j\{2S_i(u_0)-S_i(u_1)-S_i(u_2)\}, & x\neq y \end{cases}, \quad (10)$$

where $u_0 = \frac{2\pi}{\lambda}d_{xy}$. $u_1 = \frac{2\pi}{\lambda}(\sqrt{d_{xy}^2+l^2}+l)$. $u_2 = \frac{2\pi}{\lambda}(\sqrt{d_{xy}^2+l^2}-l)$. d_{xy} is the distance between the xth and yth array elements. l is the length of a dipole antenna. $C_i(\alpha) = -\int_\alpha^\infty \frac{\cos(\mu)}{\mu}d\mu$, and $S_i(\alpha) = \int_0^\alpha \frac{\sin(\mu)}{\mu}d\mu$ are the cosine and sine integrals, respectively.

Consequently, the data vector with the MC can be expressed by

$$\hat{\mathbf{x}}(t) = s_d(t)\hat{\mathbf{a}}_{MC}(\theta_d) + \sum_{j=1}^{P} s_j(t)\hat{\mathbf{a}}_{MC}(\theta_j) + \mathbf{n}(t). \quad (11)$$

3. THE PROPOSED METHOD

Here, we describe the proposed method based on the block diagram of the proposed method shown in Fig. 1. The ZF equalizer preprocesses the data vector $\mathbf{x}(t)$ received by antenna array. Then the processed data vector is inputted into the GSC-based beamforming system. After ZF equalizing, the preprocessed data vector $\hat{\mathbf{x}}_{ZF}(t) = \mathbf{A}_{ZF}\{s_d(t)\hat{\mathbf{a}}_{MC}(\theta_d)\} + \mathbf{q}(t)$ is given by

$$\hat{\mathbf{x}}_{ZF}(t) = \mathbf{A}_{ZF}\underbrace{\left(\sqrt{N}\frac{\mathbf{C}}{\|\mathbf{Ca}(\theta_d)\|}\right)}_{\text{Channel effect}}\overbrace{(s_d(t)\mathbf{a}(\theta_d))}^{\text{Preserved signal}}+\mathbf{q}(t), \quad (12)$$

where $\mathbf{A}_{ZF}$ denotes the operator of the corresponding ZF equalizer and $\mathbf{q}(t) = \mathbf{A}_{ZF}(\sum_{j=1}^{P} s_j(t)\hat{\mathbf{a}}_{MC}(\theta_j)+\mathbf{n}(t))$ interference plus noise after ZF processing.

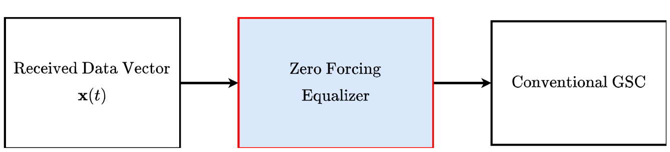

FIGURE 1. The block diagram of the proposed method.

To achieve the goal of optimally eliminating the MCE. We formulate the following optimization problem for finding the best ZF equalizer.

$$\min_{\mathbf{A}_{ZF}} \left\|\mathbf{A}_{ZF}\frac{\sqrt{N}\mathbf{C}}{\|\mathbf{Ca}(\theta_d)\|} - \mathbf{I}_N\right\|_F^2. \quad (13)$$

Since $\|\mathbf{X}\|_F = \sqrt{Tr\{\mathbf{X}\mathbf{X}^H\}}$, then the optimization problem (13) can be written as

$$\min_{\mathbf{A}_{ZF}} Tr\left\{\left(\mathbf{A}_{ZF}\frac{\sqrt{N}\mathbf{C}}{\|\mathbf{Ca}(\theta_d)\|}-\mathbf{I}_N\right)\left(\mathbf{A}_{ZF}\frac{\sqrt{N}\mathbf{C}}{\|\mathbf{Ca}(\theta_d)\|}-\mathbf{I}_N\right)^H\right\}. \quad (14)$$

Accordingly, the optimal solution of the optimization problem is given by

$$\mathbf{A}_{ZF} = \left(\sqrt{N}\frac{\mathbf{C}}{\|\mathbf{Ca}(\theta_d)\|}\right)^{-1}. \quad (15)$$

As a result, the output signal at the beamforming ouput equals $y(t) = (\mathbf{A}_{ZF}^H\mathbf{w}_{GSC})^H\hat{\mathbf{x}}(t)$, where $\mathbf{w}_{GSC}$ is given by (5).

4. PERFORMANCE ANALYSIS

In this section, we analyze the performance in terms of the SINR for the proposed robust adaptive array beamformer under mutual coupling. According to the result shown in (4) , the SINR can be expressed by

$$SINR = \frac{\mathbf{w}_{GSC}^H\left(\mathbf{A}_{ZF}\mathbf{R}_{ss}\mathbf{A}_{ZF}^H\right)\mathbf{w}_{GSC}}{\mathbf{w}_{GSC}^H\left(\mathbf{A}_{ZF}\mathbf{R}_{in}\mathbf{A}_{ZF}^H\right)\mathbf{w}_{GSC}}. \quad (16)$$

Based on the results obtained in the above section, (16) can be rewritten as

$$SINR = \frac{\sigma_d^2\left|\left(\mathbf{A}_{ZF}^H\mathbf{w}_{GSC}\right)^H\hat{\mathbf{a}}_{MC}(\theta_d)\right|^2}{\sum_{j=1}^{P}\sigma_j^2\left|\left(\mathbf{A}_{ZF}^H\mathbf{w}_{GSC}\right)^H\hat{\mathbf{a}}_{MC}(\theta_j)\right|^2+\sigma_n^2\left\|\mathbf{A}_{ZF}^H\mathbf{w}_{GSC}\right\|^2}. \quad (17)$$

According to the principle of the LCMV criteria [6], the interference components of $\hat{\mathbf{x}}_{ZF}(t)$ are negligible. Hence, the SINR of (17) is approximately equal to

$$SINR \approx \frac{\sigma_d^2\left|\mathbf{w}_{GSC}^H\left(\mathbf{A}_{ZF}\frac{\sqrt{N}\mathbf{C}}{\|\mathbf{Ca}(\theta_d)\|}\right)\mathbf{a}(\theta_d)\right|^2}{\sigma_n^2\left\|\mathbf{A}_{ZF}^H\mathbf{w}_{GSC}\right\|^2} \quad (18)$$

where $\mathbf{w}_{GSC}^H\mathbf{a}(\theta_d) = 1$ and $\mathbf{A}_{ZF}\frac{\sqrt{N}\mathbf{C}}{\|\mathbf{Ca}(\theta_d)\|} = \mathbf{I}_N$ due to the principle of ZF equalization. Moreover, since $\|\mathbf{x}\| = \sqrt{Tr\{\mathbf{x}\mathbf{x}^H\}}$, we can simplify the expression of (18) to obtain

$$SINR \approx \frac{\sigma_d^2}{\sigma_n^2}\frac{1}{Tr\left\{\mathbf{w}_{GSC}^H\mathbf{A}_{ZF}\mathbf{A}_{ZF}^H\mathbf{w}_{GSC}\right\}}. \quad (19)$$

Since $Tr\{\mathbf{XY}\} = Tr\{\mathbf{YX}\}$, $Tr\{\mathbf{XY}\} \leq \sqrt{Tr\{\mathbf{X}^H\mathbf{X}\}}\sqrt{Tr\{\mathbf{Y}^H\mathbf{Y}\}}$ and $\|\mathbf{X}\|_F = \sqrt{Tr\{\mathbf{X}^H\mathbf{X}\}}$, then the denominator of (19) can be rewritten by

$$Tr\left\{\mathbf{w}_{GSC}^H\mathbf{A}_{ZF}\mathbf{A}_{ZF}^H\mathbf{w}_{GSC}\right\} \leq \|\mathbf{w}_{GSC}\|^2\|\mathbf{A}_{ZF}\|_F^2, \quad (20)$$

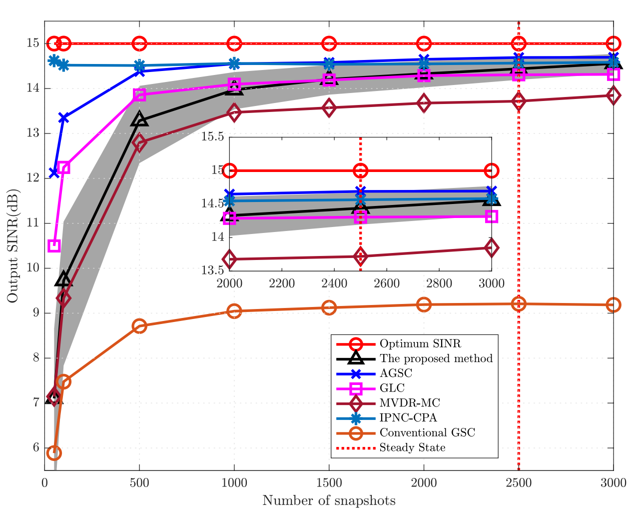

FIGURE 2. The output SINR versus the number of snapshots for Example 1.

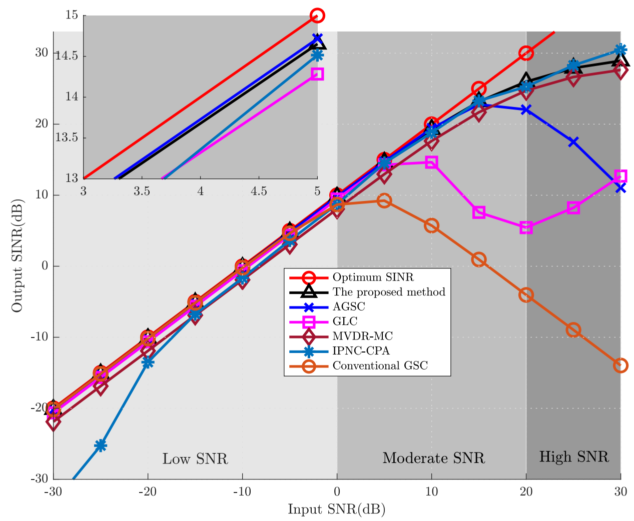

FIGURE 3. The output SINR versus the input SNR for Example 1.

where $\|\mathbf{w}_{GSC}\|^2 = \frac{1}{N}$. Then, the lower bound can be given by

$$N\frac{\sigma_d^2}{\sigma_n^2}\frac{1}{\|\mathbf{A}_{ZF}\|_F^2} \leq SINR. \tag{21}$$

As we know, the optimum SINR performance for adaptive beamforming is constrained by $N\frac{\sigma_d^2}{\sigma_n^2}$. Therefore, the range of the beamforming performance of the proposed method is given by

$$\frac{N\sigma_d^2}{\sigma_n^2\left(\sum_{q=1}^{N}\sum_{k=1}^{N} a_{q,k}a_{k,q}^*\right)} \leq SINR < N\frac{\sigma_d^2}{\sigma_n^2}, \tag{22}$$

where $a_{x,y}$ denotes (x,y)th entries of $\mathbf{A}_{ZF}$.

5. SIMULATION RESULTS

In this section, simulation results performed on a PC using Matlab programming language are presented for illustration. All simulation results are obtained by averaging 100 Monte Carlo runs. For illustration and comparison, several notable methods, such as conventional GSC beamformer [7], advanced GSC (AGSC) based method [10], the method of [16] (IPNC-CPA), the method of general linear combination technique (GLC) [20], and the MVDR method of [14] (MVDR-MC) are also performed. Due to that the correlation matrix $\mathbf{R}_{xx}$ is not available in practical situations, the sample correlation matrix $\hat{\mathbf{R}}_{xx}$ instead of $\mathbf{R}_{xx}$ is utilized for performing all simulations. The sample correlation matrix $\hat{\mathbf{R}}_{xx}$ is computed as follows

$$\hat{\mathbf{R}}_{xx} = \frac{1}{L}\sum_{k=0}^{L-1}\mathbf{x}(k)\mathbf{x}(k)^H, \tag{23}$$

where L is the number of sample snapshots used and $\mathbf{x}(k)$ is the received data vector taken at the kth time instant. The order K_{AGSC} of the additional derivative constraint matrix adopted by the AGSC is set to $K_{AGSC} = 4$.

5.1. Example 1

In this case, the GSC-based beamforming system is deployed by a ULA with 10 antenna elements having interelement spacing equal to half of the minimum wavelength λ of signals. There are four signals impinging on the array from $\theta_d = 0°$, $\theta_1 = -35°$, $\theta_2 = -25°$, and $\theta_3 = 20°$, respectively, off array broadside. Moreover, the first one signal is assumed to be the desired signal and the others are interference with interference-to-noise ratio (INR) equal to 10 dB.

Figure 2 plots the output SINR versus the number of data snapshots under SNR = 5 dB. The dashed vertical line indicates the situation at "steady-state" snapshot count. The horizontal line shows the theoretical limit, namely the optimal SINR bound. The shaded regions in the figure provide the ± 1 standard deviation in terms of the statistical representation over multiple trials. The output SINR versus the input SNR of the desired signal is shown in Fig. 3. L is set to 5000. Fig. 4 depicts the beampattern versus the spatial angles θ. L and SNR are set to 5000 and 10 dB, respectively.

From Figs. 2, 3, and 4, we note that the proposed method processes the better performance than the others under MC effect.

5.2. Example 2

In this case, a ULA with 12 antenna elements having interelement spacing equal to half of the minimum wavelength λ of signals is employed for beamforming. There are six signals impinging on the array from $\theta_d = 0°$, $\theta_1 = -35°$, $\theta_2 = -10°$, $\theta_3 = 10°$, $\theta_4 = 25°$, and $\theta_5 = 30°$, respectively, off array broadside. Again, the first signal is assumed to be the desired signal and the others are interference that interference-to-noise ratio (INR) is fixed at 10 dB.

Figure 5 plots the output SINR versus the number of data snapshots. The SNR is set to 5 dB. The output SINR versus the input SNR of the desired signal is depicted in Fig. 6. L is set to 5000. The beampattern versus the spatial angles θ is shown

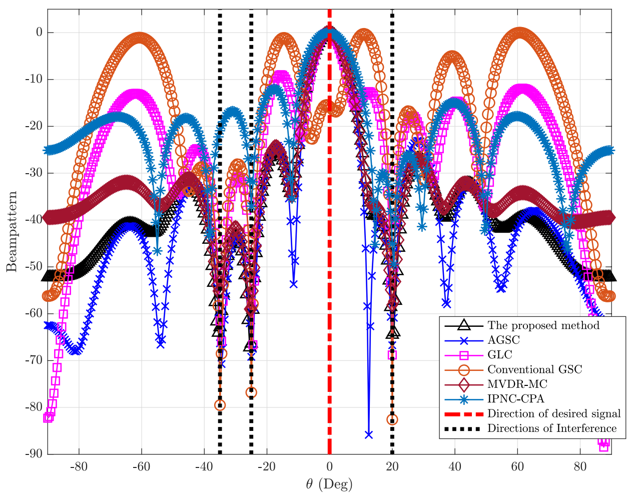

FIGURE 4. The beampattern versus the spatial angle θ for Example 1.

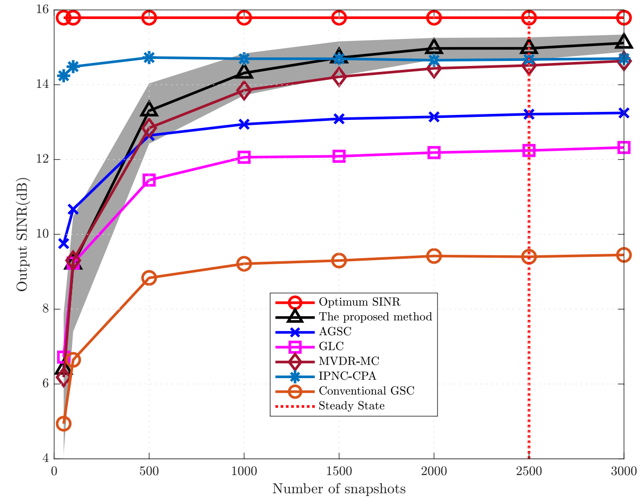

FIGURE 5. The output SINR versus the number of snapshots for Example 2.

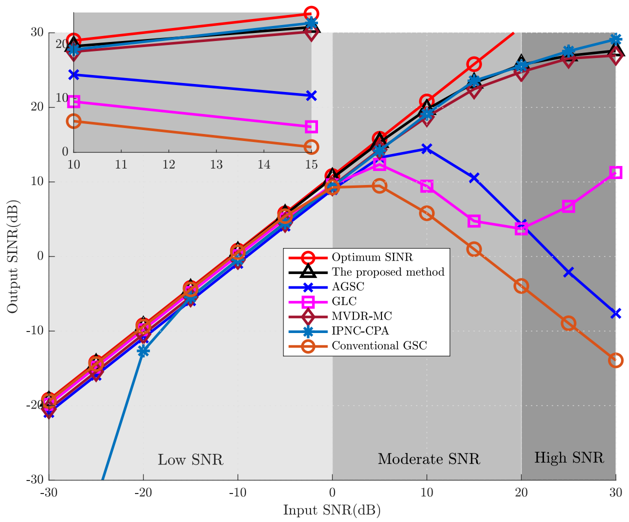

FIGURE 6. The output SINR versus the input SNR for Example 2.

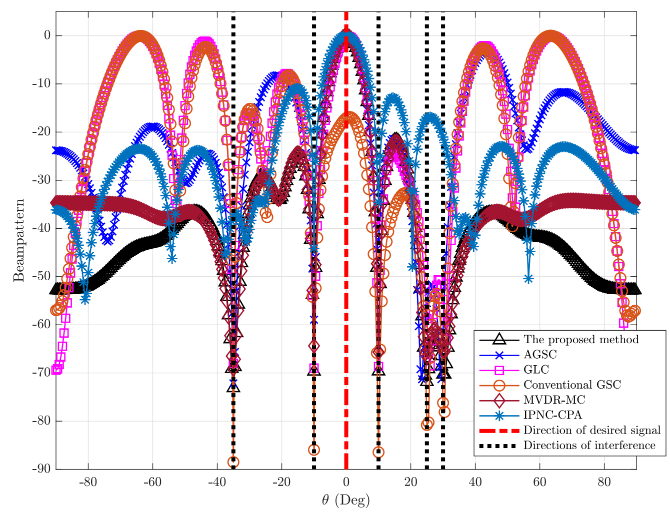

FIGURE 7. The beampattern versus the spatial angle θ for Example 2.

in Fig. 7. L and SNR are set to 5000 and 10 dB, respectively. These three figures demonstrate that the proposed method outperforms the other methods in this case.

From the simulation results, we can see that the proposed method provides better performance due to the utilization of a ZF equalizer. The superiority of using the proposed method mainly comes from that ZF equalizer preprocesses the received data vector to provide a cure for MC effect. Then, we adopt the conventional GSC based array beamformer to effectively cope with the enhanced noise due to ZF equalizer.

6. CONCLUSION

We have presented an efficient method to cope with the performance degradation of adaptive array beamforming due to the effect of array mutual coupling. The proposed method exploits the principle of a well-known ZF equalizer to achieve robust beamforming. The ZF equalizer preprocesses the received data vector and then inputs the processed data vector into the adaptive GSC based beamforming system. The novelty of the proposed method is that a ZF equalizer cooperates with a GSC-based adaptive beamformer to achieve robust adaptive beamforming. The capability of a ZF equalizer in suppressing the channel effect as well as the inter-symbol-interference (ISI) for wireless communication systems under multipath environment is utilized to effectively mitigate the mutual coupling effect between array elements. The superiority of a GSC based adaptive beamformer is employed for suppressing interference and noise. As a result, the proposed method provides robustness against the effect of array mutual coupling without resorting to robust algorithms and sacrificing computation complexity for adaptive beamforming. The performance analysis of the proposed method has been analyzed. Simulation results have been presented for confirming effectiveness and making comparison. From the simulation results shown by the figures, we note that the proposed method outperforms the existing robust methods. Based on this achievement, an interesting future work is to enhance the performance of the proposed method by developing a more appropriate GSC-based adaptive beamformer instead of the current one.

ACKNOWLEDGEMENT

This work was supported by the National Science and Technology Council of Taiwan under Grant NSTC 113-2221-E-002-147.

REFERENCES

[1] Richards, M. A., J. A. Scheer, and W. A. Holm, *Principles of Modern Radar: Basic Principles*, IET, 2010.

[2] Wada, Y., H. Kikuchi, E. Yoshikawa, D. Kitahara, and T. Ushio, "Phase and amplitude correction for adaptive beamforming of phased array weather radar," *IEEE Transactions on Geoscience and Remote Sensing*, Vol. 62, 1–11, 2024.

[3] Peng, C., L. Wang, J. Gao, S. Zhang, and H. Ji, "A new active sonar detector based on beamformed deep neural network," *IEEE Journal of Oceanic Engineering*, Vol. 50, No. 2, 1370–1386, 2025.

[4] Kashikar, R., "Quantum AI-enhanced deep reinforcement learning for real-time adaptive beamforming in next-generation terahertz communication systems," in *2025 International Conference on Artificial Intelligence in Information and Communication (ICAIIC)*, 0238–0242, Fukuoka, Japan, 2025.

[5] Wu, K., J. A. Zhang, and Y. J. Guo, *Joint Communications and Sensing: From Fundamentals to Advanced Techniques*, John Wiley & Sons, 2022.

[6] Frost, O. L., "An algorithm for linearly constrained adaptive array processing," *Proceedings of the IEEE*, Vol. 60, No. 8, 926–935, 1972.

[7] Griffiths, L. and C. Jim, "An alternative approach to linearly constrained adaptive beamforming," *IEEE Transactions on Antennas and Propagation*, Vol. 30, No. 1, 27–34, 1982.

[8] Breed, B. R. and J. Strauss, "A short proof of the equivalence of LCMV and GSC beamforming," *IEEE Signal Processing Letters*, Vol. 9, No. 6, 168–169, 2002.

[9] Wang, C.-J. and J.-H. Lee, "Generalized sidelobe canceller based antenna array beamformer with reduced computational complexity," in *Proceedings of SAI Intelligent Systems Conference*, 845–856, 2023.

[10] Wang, C.-J. and J.-H. Lee, "Generalized sidelobe canceller based adaptive multiple-input multiple-output radar array beamforming under scenario mismatches," *Signal Processing*, Vol. 227, 109739, 2025.

[11] Wang, C.-J. and J.-H. Lee, "Robust adaptive multiple-input multiple-output radar array beamforming using advanced generalized sidelobe canceller against random scenario mismatches," *IEEE Access*, Vol. 13, 125 383–125 396, 2025.

[12] Jemaludin, N. H., A. J. A. Al-Gburi, R. H. Elabd, T. Saeidi, M. F. Akbar, I. M. Ibrahim, and Z. Zakaria, "A comprehensive review on MIMO antennas for 5G smartphones: Mutual coupling techniques, comparative studies, SAR analysis, and future directions," *Results in Engineering*, Vol. 23, 102712, 2024.

[13] Ihrayz, E. A. M. B., "Mutual coupling effect on spectral efficiency of 5G massive MIMO millimeter wave antenna array," *Open Journal of Energy Efficiency*, Vol. 13, No. 4, 101–119, 2024.

[14] Boughaba, N., C. Chettah, and O. Barkat, "Adaptive beamforming algorithm based on MVDR for smart linear dipole array with known mutual coupling," *Progress In Electromagnetics Research C*, Vol. 124, 125–134, 2022.

[15] Lee, J.-H. and Y.-X. Li, "Multiple-input multiple-out radar robust beamforming under unknown array mutual coupling," in *2023 IEEE 5th Eurasia Conference on IOT, Communication and Engineering (ECICE)*, 100–104, Yunlin, Taiwan, 2023.

[16] Chen, L.-H. and J.-H. Lee, "Robust MIMO radar adaptive beamforming with coprime array under mismatch scenarios," in *2024 IEEE 4th International Conference on Electronic Communications, Internet of Things and Big Data (ICEIB)*, 758–762, Taipei, Taiwan, 2024.

[17] Lin, Y.-P., S.-M. Phoong, and P. P. Vaidyanathan, *Filter Bank Transceivers for OFDM and DMT Systems*, Cambridge University Press, 2010.

[18] Svantesson, T., "Modeling and estimation of mutual coupling in a uniform linear array of dipoles," in *1999 IEEE International Conference on Acoustics, Speech, and Signal Processing. Proceedings. ICASSP99 (Cat. No.99CH36258)*, Vol. 5, 2961–2964, Phoenix, AZ, USA, 1999.

[19] Durrani, S. and M. E. Bialkowski, "Effect of mutual coupling on the interference rejection capabilities of linear and circular arrays in CDMA systems," *IEEE Transactions on Antennas and Propagation*, Vol. 52, No. 4, 1130–1134, 2004.

[20] Ali, M. F., M. S. Hossain, and M. M. Rashid, "Robust antenna array processor in the presence of steering angle mismatch and mutual coupling effect," in *2015 IEEE International Conference on Telecommunications and Photonics (ICTP)*, 1–5, Dhaka, Bangladesh, 2015.